Biogeosciences Discuss., 10, 6861–6898, 2013
www.biogeosciences-discuss.net/10/6861/2013/
doi:10.5194/bgd-10-6861-2013

Biogeosciences Discussions
Open Access

Technical Note: Simultaneous measurement of sedimentary N_2 and N_2O production and new ^{15}N isotope pairing technique

T.-C. Hsu[1] **and S.-J. Kao**[1,2]

[1]Earth System Science Program, Taiwan International Graduate Program, Research Center for Environmental Changes, Academia Sinica, Taipei, Taiwan
[2]State Key Laboratory of Marine Environmental Science, Xiamen University, Xiamen, China

Received: 31 March 2013 – Accepted: 4 April 2013 – Published: 17 April 2013

Correspondence to: S.-J. Kao (sjkao@gate.sinica.edu.tw)

Published by Copernicus Publications on behalf of the European Geosciences Union.

Abstract

Dinitrogen (N_2) and/or nitrous oxide (N_2O) are produced through denitrification, anaerobic ammonium oxidation (anammox) or nitrification in sediments, of which entangled processes obfuscate the absolute rate estimation of gaseous nitrogen production from individual pathway. Recently, the classical isotope pairing technique (IPT), the most common ^{15}N-nitrate enrichment method to quantify denitrification, has been modified by different researchers to (1) discriminate relative contribution of N_2 production by denitrification from anammox or to (2) provide more accurate denitrification rate by considering both N_2O and N_2 productions. Both modified methods, however, have deficiencies such as overlooking N_2O production in case 1 and neglecting anammox in case 2. In this paper, a new method was developed to refine previous methods. We installed cryogenic traps to pre-concentrate N_2 and N_2O separately, thus, allowing simultaneous measurement for two gases generated by one sample. The precision is better than 2 % for N_2 (*m/z* 28, *m/z* 29 and *m/z* 30), and 1.5 % for N_2O (*m/z* 44, *m/z* 45 and *m/z* 46). Based on the six *m/z* peaks of the two gases, we further revised IPT formulae to truthfully resolve the production rates of N_2 and N_2O contributed from 3 specific nitrogen removal processes, i.e. N_2 and N_2O from denitrification, N_2 from anammox and N_2O from nitrification. To validate the applicability of our new method, incubation experiments were conducted using sediment cores taken from the Danshuei estuary in Taiwan. We successfully determined the rates of aforementioned nitrogen removal processes. Moreover, N_2O yield was as high as 66 %, which no doubt would significantly bias previous IPT approaches when N_2O was not considered. Our new method not only complements the previous IPT but also provides more comprehensive information to advance our understanding of nitrogen dynamics through the water-sediment interface.

BGD
10, 6861–6898, 2013

1 Introduction

Nitrate as fertilizer which ends up in the environment, polluting waterways and the coastal zone, or accumulating in land systems, will be transformed to N_2 and N_2O gases via denitrification, anammox and nitrification processes in sub-anoxic conditions, may get removed from the environment (Joye and Anderson, 2008). Net production of N_2O, which is a strong greenhouse gas, from ocean accounts for 1/3 of atmospheric N_2O flux (Bange, 2006). The N_2O production may rise further as a result of increasing anthropogenic nitrogen input, exacerbating coastal eutrophication and global warming (Naqvi et al., 2010). Sediment-water interface is a major locus for nitrogen removal in aquatic environment. To better predict the future nitrogen cycle, it is critical explore the processes and regulation factors for nitrogen removal and N_2O emission through the sediment-water interface.

The ^{15}N tracer based methods have been applied widely in nitrogen cycle studies in terrestrial and aquatic environments (Groffman et al., 2006). It is a straightforward method to quantify denitrification rates by adding ^{15}N-labeled NO_3^- ($^{15}NO_3^-$) and measuring the gaseous production after incubations. Since both ^{15}N-labeled N_2 ($^{15}N_2$) and/or N_2O ($^{15}N_2O$) will be generated at the same time, simultaneous analysis of $^{15}N_2$ and $^{15}N_2O$ is critical to single out individual contributing process from complicated nitrogen reaction web. However, to our knowledge, dual measurement has not yet been made in aquatic environments due to method difficulties, though a few were conducted in soil studies (Bergsma et al., 2001; Spott et al., 2006; Stevens et al., 1993).

In aquatic environment, ^{15}N-nitrate enrichment technique, i.e. the isotope pairing technique (IPT), is oft-used to study nitrate removal processes. After the original version of IPT by Nielsen (1992), several modified versions were proposed to accommodate anammox or to resolve specific nitrogen removal processes in sediments (Fig. 1). The original version of IPT ($IPT_{classic}$, yellow plate in Fig. 1) was used to estimate the genuine N_2 gas production rate ($P_{14\text{-classic}}$) which was defined as an estimate of $^{14}N_2$ production as it would have occurred without the addition of ^{15}N tracer, i.e. N_2

BGD
10, 6861–6898, 2013

production by reactions utilizing $^{14}NO_3^-$. This method can separate the denitrification supported by water column NO_3^- from coupled nitrification denitrification; yet, the recently discovered anammox is not included. Based on the $IPT_{classic}$, Risgaard-Petersen et al. (2003) and Trimmer et al. (2006) proposed IPT_{ana} enabling the estimation of anammox (yellow and blue plates in Fig. 1). Unfortunately, all above methods did not take N_2O production into account. During the same period, Master et al. (2005) brought up an alternative approach, IPT_{N_2O}, which considered both N_2 and N_2O from denitrification (see pink and yellow plates in Fig. 1), yet, anammox was missing in their method. Meanwhile, they focused on theory providing no experimental data.

In this study we designed a pre-concentration system to trap and release N_2O and N_2 separately for isotope measurements. To overcome aforementioned shortages we re-assemble the formulae of former versions of IPT. Our new IPT_{anaN_2O} considers both N_2O production and anammox allowing us to determine the absolute rate of each individual N removal pathway in complicated transformation processes, thus, to project better insights into the full scheme of the nitrogen reaction web (Fig. 1).

2 Instrument setup and evaluations

A program control trap-and-release preparation line was constructed and connected to IRMS to facilitate the simultaneous quantification of stable isotope compositions of N_2 and N_2O extracted from a single vial. Since the concentration of N_2 is often 3 to 5 orders of magnitude higher than N_2O in aquatic environments, we need to maximize the analytical capacity of our instrument system. Three extra head amplifiers were added onto detectors in IRMS to widen the detection range, meanwhile, an adjustable N_2 divider (open split to atmosphere) was installed in the preparation system to reduce N_2 inflow into the IRMS. Through this modified system, the genuine production of N_2 and N_2O from denitrification and anammox ($P_{14\text{-}anaN_2O}$) i.e. ^{14}N–N_2 and ^{14}N–N_2O production rate as it would have occurred without the addition of $^{15}NO_3^-$, can be obtained from

BGD
10, 6861–6898, 2013

the new IPT formulae. The rate of N_2O formation via nitrification could be estimated as well.

2.1 Pre-concentration system and instrument modification

The pre-concentration system (Fig. 2) was added onto an existing combination of equipment including a GC-Pal autosampler (CTC analytics, LEAP Technologies), a GasBench II embedded with a PoraPlot Q GC column (25 m) and an IRMS (Thermo Delta^{plus} Advantage). The sample preparation line composed of three two-position rotary valves (V1-V3, Vivi Valco prod. No. A4C8WT), which are program-controlled by Isodat software. We followed McIlvin and Casiotti (2010) to utilize the two-way concentric needle for the autosampler to flush and retrieve gases out of the vial. Although two Nafion gas dehumidifying tubes had been installed originally by the manufacturer on GasBench II, we added an extra chemical column (12 inches glass tube, 3/8-inch i.d. and 1/2-o.d.) packed with magnesium perchlorate and Ascarite II (Fisher) to ensure a complete remove of water moisture and CO_2. The N_2 "gas divider" is a Valco tee (1/16-inch tubing o.d.) with a changeable fused silica tube outlet (0.32 mm i.d.). The dividing ratio is 95/5 thus 95 % gas stream flows out of the system. The dividing ratio can be adjusted by changing the flow rate of the fused silica tube outlet (O3). The N_2 and N_2O traps were made of a stainless steel tube (40 cm long 1/16-inch o.d and 0.04 inch i.d.) in U shape, one of them filled with nickel wires and the other with molecular 5 Å sieve (60/80 granular, GRACE), respectively. In our system, N_2O is bypassing the copper furnace, i.e. N_2O is measured non-destructively so the bias caused by reduction reaction (N_2O or NO to N_2) can be avoided. The standard gas is a mixture of N_2 and N_2O (2000 ppm and 100 ppm, respectively). In the preparation system, sample gas flows through the fused silica tube (430 µm o.d.; 320 µm i.d.) and the standard and carrier gases flow through the stainless steel tube (1/16-inch o.d.; 0.04-inch i.d.).

The analytical procedure includes three phases, sample loading, N_2 injection and N_2O injection. In sample loading phase, helium gas (99.999 % purity) gets to the bottom of the sample vial bubbling gases out of the slurry to the sample preparation line.

BGD
10, 6861–6898, 2013

A complete extraction of N_2 and N_2O contained in the vial would take 5 min at a flow rate of 21 mL min^{-1} (O3 + O5). The gas sample flows through chemical column while V1 is at "sample" position (Fig. 2). After the second dehumidification by Nafion tube membrane the gas sample will get into the two cryogenic traps. N_2O will be captured, concentrated and retained when the first trap submerged in liquid nitrogen. The trapping efficiency of N_2O is better than 95 % validated by standard gas. N_2 will be trapped in the second trap assembled on V3. In between the two traps a copper oxidation furnace fixed at 600 °C was installed to remove O_2 in the flowing stream and to convert trace NO_x into N_2. The gas divider allows 5 % target gas to be trapped thus ensures that N_2 would not surpass the detection range of IRMS.

In N_2 injection phase, N_2 trap was pulled up and heated to 300 °C in 20 s to release captured N_2. At the same time, V3 was switched to "injection" mode to allow helium gas (flow rate of 2 mL min^{-1} for 3 min) to flush N_2 through the GC column and Nafion membrane and then into IRMS. After N_2 injection phase was completed, N_2O trap was elevated above LN_2, and then V2 and V3 were switched to "injection" and "loading" position for 7 min, respectively, in room temperature to release N_2O. In the meantime, the preparation line was back-flushed for cleaning by two helium gas streams mounted on V2.

On the other hand, in highly enriched ^{15}N tracer study the target gases frequently give signals exceeding the normal range of IRMS detectors. Besides the original resistors on amplifiers (3×10^8, 3×10^{10} and 1×10^{11} Ω), we added a second set of resistors 3×10^{10}, 3×10^8 and 3×10^8 Ω onto cup 1, 2 and 3, respectively. Combining the N_2 divider with the second sets of resistor in IRMS our system is now capable of detecting a wide range of ^{15}N tracer. The entire design let us get the signal of *m/z* 44, which represents the absolute amount of N_2O. After proper calibration by using standard gases this signal can be applied to advance IPT calculation.

BGD
10, 6861–6898, 2013

2.2 Validation of instrument modifications

The reproducibility and linearity of IRMS signals are critical to obtain accurate results. In our system, the most significant instrument modification is the two additional cryogenic sample traps and the gas divider. We applied three kinds of validation for verification. By changing different length of STD loop (Fig. 2) different volumes of standard gas (mixture of N_2 and N_2O) were used for calibration. The linear responses ($r^2 = 1$ for all) were shown in signal areas of *m/z* 28, 29 and 30 over the range from 2 to 32 µmol for N_2 and areas of *m/z* 44, 45 and 46 over the range from 4 to 83 nmol for N_2O (Fig. 3). Good signal area reproducibility could be judged from small relative standard deviation for N_2 (between 1.5 % to 2.3 % in three isotopic species, $n = 70$) and for N_2O (below 1.5 % in three isotopic species, $n = 80$). Constant ratios for *m/z* 29/28, *m/z* 30/28, *m/z* 45/44 and *m/z* 46/44 were observed throughout the calibrations. Note that in Fig. 3a, a N_2 background signal (intercept 7.75 µmol in $^{28}N_2$) was observed; yet such signal was expected and would neither affect the calculation of excess ^{15}N ratio (1992) nor the production of $^{29}N_2$ and $^{30}N_2$. The trap efficiency was further tested by injecting a given amount of standard gas mixture, which was passing through the preparation line freely without trapping. These signals were compared with those under operation of cryogenic traps. Results showed that we have high and stable trapping efficiency for N_2 and N_2O over wide range signal (> 90 %). In the third batch validation, we used different volumes of water in saturation with standard gas mixture to check the recovery of signal after passing through the entire procedure. The results (not shown) are very good as expected again showing consistent trap efficiencies and a stable dividing ratio of the gas divider throughout all measurements.

Meanwhile, we validated the reliability of the additional amplification factors by cross-checking signals provided by the two amplifiers of the same cup with a given amount of N_2 gas. The results of the three cups gave consistency after signal conversion (*t* test, $p > 0.5$, $n = 15$). The conversion factor agreed perfectly with the expected amplification factor.

BGD
10, 6861–6898, 2013

3 Development of IPT

3.1 Reported IPT estimators

The critical parameter in IPT is r_{14} (Fig. 1), an estimation ratio between $^{14}NO_3^-$ and $^{15}NO_3^-$ undergoing denitrification in the nitrate reduction layer. In $IPT_{classic}$ proposed by Nielsen[8], r_{14} was derived from the production rates of $^{29}N_2$ (P_{29}) and $^{30}N_2$ (P_{30}) as

$$r_{14\text{-}N_2} = \frac{P_{29}}{2 \cdot P_{30}}. \quad (1)$$

There are three major assumptions behind the above equation: (1) production rates of isotopic nitrogen gases species (i.e. $^{28}N_2$, $^{29}N_2$ and $^{30}N_2$ in $IPT_{classic}$; $^{44}N_2O$, $^{45}N_2O$ and $^{46}N_2O$ in other versions of IPT) obey binomial distribution, (2) the ratio between $^{14}NO_3^-$ and $^{15}NO_3^-$ is constant in the NO_3^- reduction zone and (3) denitrification is the only pathway for $^{15}N\text{–}N_2$ production (see Sect. 4.3 for detail); thus, the isotope composition of N_2 should reflect that of the reduced NO_3^-. The genuine N_2 production from denitrification ($P_{14\text{-classic}}$ or $D_{14\text{-classic}}$, see Fig. 1) is estimated as

$$P_{14\text{-classic}} = D_{14\text{-classic}} = r_{14\text{-}N_2} \cdot (2 \cdot P_{30} + P_{29}), \quad (2)$$

where the suffix N_2 denotes parameters derived solely from $^{15}N\text{–}N_2$ production rates (upcoming $r_{14\text{-}N_2O}$ and $D_{14\text{-}N_2O}$ refer to $^{15}N_2O$).

Anammox also produces N_2 as denitrification does, yet the two atoms of N in N_2 from anammox are sourced from NH_4^+–N and NO_2–N in 1 to 1 mole ratio (van de Graaf et al., 1997). This recently-discovered nitrogen removal process (Mulder et al., 1995) was of course not included in the $IPT_{classic}$ when it was proposed. The presence of anammox violates the basic assumptions of $IPT_{classic}$ and causes overestimation in $D_{14\text{-classic}}$, which was explained clearly by Risgaard-Petersen et al. (2003). Accordingly, a revised

BGD
10, 6861–6898, 2013

version of IPT (IPT_{ana}) was recommended to properly estimate the genuine N_2 production ($P_{14\text{-ana}}$) from anammox and denitrification in sediments (Risgaard-Petersen et al., 2003).

Similar to $IPT_{classic}$, ^{15}N-nitrate enrichment in intact sediment core incubations and direct measurement of P_{29} and P_{30} were conducted in IPT_{ana} method. However, Risgaard-Petersen et al. (2003) introduced two indirect approaches to derive r_{14}. The first approach requires additional slurry incubation by adding $^{15}NH_4^+$ to measure the proportional contribution of anammox to the total N_2 production (*ra*). The second approach requires additional sets of sediment core incubation, by which a linear relationship of $^{15}N_2$ production rates against $^{15}NO_3^-$ enrichment gradients can be generated to eliminate anammox-biased r_{14} indirectly.

Trimmer et al. (2006) suggested using ^{15}N–N_2O to derive r_{14} ($r_{14\text{-}N_2O}$) to avoid the bias from anammox. When anammox exists, P_{29} (Fig. 1) is contributed partially from anammox ($^{14}NH_4^+ + {}^{15}NO_2$), $r_{14\text{-}N_2}$ is hence improper to represent $^{14}N/^{15}N$ ratio of NO_3^- reduced by denitrifier. Since ^{15}N–N_2O was only sourced from denitrification the $r_{14\text{-}N_2O}$ is thus more representative and no longer influenced by anammox (Trimmer et al., 2006). Similarly, the distribution of $^{15}N_2O$ isotopic species will follow the fundamental assumptions of $IPT_{classic}$ regarding the distribution of ^{15}N–N_2 isotopic species and can be used to estimate r_{14} as

$$r_{14\text{-}N_2O} = \frac{P_{45}}{2 \cdot P_{46}}, \tag{3}$$

where P_{45} and P_{46} are the production rates of $^{45}N_2O$ and $^{46}N_2O$. According to Risgaard-Petersen et al. (2003) the genuine N_2 production ($P_{14\text{-ana}}$) can be expressed as

$$P_{14\text{-ana}} = D'_{14\text{-}N_2} + A_{14}, \tag{4}$$

where $D'_{14\text{-}N_2}$ and A_{14} represent the genuine N_2 production, respectively, from denitrification and anammox (Fig. 1). Accordingly, $D'_{14\text{-}N_2}$ and A_{14} can be expressed in terms

BGD
10, 6861–6898, 2013

of measurable parameters, $r_{14\text{-}N_2O}$, P_{29} and P_{30}:

$$D'_{14\text{-}N_2} = (r_{14\text{-}N_2O} + 1) \cdot 2 \cdot r_{14\text{-}N_2O} \cdot P_{30} \quad (5)$$

and

$$A_{14} = 2 \cdot r_{14\text{-}N_2O} \cdot (P_{29} - 2 \cdot r_{14\text{-}N_2O} \cdot P_{30}), \quad (6)$$

where the formula, $P_{29} - 2 \cdot r_{14\text{-}N_2O} \cdot P_{30}$, represents the anammox N_2 production by utilizing $^{15}NO_3^-$ (A_{15}). Substituted by Eqs. (5) and (6), $P_{14\text{-ana}}$ becomes

$$P_{14\text{-ana}} = 2 \cdot r_{14\text{-}N_2O} \cdot [P_{29} + P_{30} \cdot (1 - r_{14\text{-}N_2O})]. \quad (7)$$

On the other hand, based on Neilsen's $IPT_{classic}$ (1992), Master et al. (2005) proposed that IPT_{N_2O} ought to include the rate of N_2O production in the total denitrification rate; nevertheless, they ignored anammox (Fig. 1). According to their assumption, denitrification is the only NO_3^- reduction process to be considered in IPT_{N_2O}, the distribution of $^{15}N_2$ and $^{15}N_2O$ isotopic species should be equal and is expressed as:

$$r_{14\text{-}N_2} = r_{14\text{-}N_2O}. \quad (8)$$

Thus, IPT_{N_2O} estimates the genuine N_2 and N_2O production from denitrification ($D_{14\text{-}N_2}$ and $D_{14\text{-}N_2O}$, respectively, see Fig. 1) by the following equation:

$$\begin{aligned} P_{14\text{-}N_2O} &= D_{14\text{-}N_2} + D_{14\text{-}N_2O} \\ &= r_{14\text{-}N_2O} \cdot (2 \cdot P_{30} + P_{29}) + r_{14\text{-}N_2O} \cdot (2 \cdot P_{46} + P_{45}) \\ &= r_{14\text{-}N_2O} \cdot (2 \cdot P_{30} + P_{29} + 2 \cdot P_{46} + P_{45}). \end{aligned} \quad (9)$$

BGD
10, 6861–6898, 2013

3.2 Newly proposed IPT method

As mentioned earlier, previous reported IPT methods have flaws in various ways. Since we can precisely measure both N_2 and N_2O after incubation, we are now proposing a new IPT ($IPT_{ana N_2O}$) estimator, which is an integration of IPT_{ana} and IPT_{N_2O} that is able to complete estimations of gaseous nitrogen production in ^{15}N-nitrate enriched experiments.

$IPT_{ana N_2O}$ involves the production of (1) N_2 from denitrification, (2) N_2 from anammox, (3) N_2O from denitrification and (4) N_2O from nitrification, thus, representing a combination of IPT_{ana} and IPT_{N_2O} as shown in Fig. 1. The parameters, $D'_{14\text{-}N_2}$, A_{14}, $D_{14\text{-}N_2O}$ in the proceeding equations can be derived independently. Therefore, the accurate total genuine N_2 and N_2O production ($P_{14\text{-}ana N_2O}$) from all related processes can be summarized as:

$$\begin{aligned} P_{14\text{-}ana N_2O} &= D'_{14\text{-}N_2} + A_{14} + D_{14\text{-}N_2O} \\ &= (r_{14\text{-}N_2O} + 1) \cdot 2 \cdot r_{14\text{-}N_2O} \cdot P_{30} + 2 \cdot r_{14\text{-}N_2O} \cdot (P_{29} - 2 \cdot r_{14\text{-}N_2O} \cdot P_{30}) \\ &\quad + r_{14\text{-}N_2O} \cdot (2 \cdot P_{46} + P_{45}) \\ &= 2 \cdot r_{14\text{-}N_2O} \cdot [P_{29} + P_{30}(1 - r_{14\text{-}N_2O})] + r_{14\text{-}N_2O} \cdot (2 \cdot P_{46} + P_{45}). \end{aligned} \quad (10)$$

Similar to Risgaard-Petersen et al. (2003) the $P_{14\text{-}ana N_2O}$ can be further separated into two components (1) the genuine N_2 and N_2O production supported by water column delivered nitrate ($P_{14}w$) and (2) the genuine N_2 and N_2O production supported via coupled nitrification denitrification ($P_{14}n$):

$$P_{14}w = P_{14\text{-}ana N_2O} \cdot \frac{r_{14}w}{r_{14\text{-}N_2O}} \quad (11)$$

$$P_{14}n = P_{14\text{-}ana N_2O} - P_{14}w = P_{14\text{-}ana N_2O} \cdot \left(1 - \frac{r_{14}w}{r_{14\text{-}N_2O}}\right), \quad (12)$$

BGD
10, 6861–6898, 2013

where $r_{14}w$ is the ratio of $^{14}NO_3^-$ to $^{15}NO_3^-$ in the water column.

Another crucial parameter, *ra*, which can be used to separate fractional contribution of N_2 from anammox, can also be obtained. According to Risgaard-Petersn et al. (2003), *ra* is expressed as

$$ra = \frac{A_{14}}{D'_{14\text{-}N_2} + A_{14}}. \quad (13)$$

Trimmer et al. (2006) suggested an alternative approach to derive *ra* after completing $^{15}NO_3^-$ concentration series experiments (see below). According to Trimmer et al. (2006), the term r_{14} is converted into another parameter,

$$q = \frac{1}{r_{14} + 1}, \quad (14)$$

where q is the proportion of ^{15}N in the NO_3^- pool undergoing denitrification. Since r_{14} can be derived from $^{15}N_2$ or $^{15}N_2O$, the qN_2 is directly related to $r_{14\text{-}N_2}$ and the qN_2O is related to $r_{14\text{-}N_2O}$. By using regression analysis, the slope of the qN_2 against qN_2O derived from $^{15}NO_3^-$ concentration series incubations can form an equation for *ra*:

$$ra = \frac{2 - 2 \cdot \text{slope}}{2 - \text{slope}}. \quad (15)$$

We specifically clarify that mathematically the value of *ra* derived from Eq. (13) is equal to that from Eq. (15) because both equations might be misled from different methods (see Appendix A). However, the benefit of Eq. (15) is that through $^{15}NO_3^-$ concentration series incubations we can directly derive the average *ra* from the plot of the qN_2 vs. qN_2O (e.g. Fig. 5). Unfortunately, both above *ra* estimations did not consider N_2O produced by denitrification.

As Master et al. (2005) described, N_2O produced by nitrification can be derived by calculation. Theoretically, the $^{44}N_2O$ measured directly by IRMS ($[D_{44} + P'_{44}]_{IRMS}$) is

BGD
10, 6861–6898, 2013

composed of two components, the $^{44}N_2O$ formation via nitrification (P'_{44}) and denitrification (D_{44}). Accordingly, P'_{44} can be expressed as:

$$P'_{44} = [D_{44} + P'_{44}]_{\mathrm{IRMS}} - D_{44}, \tag{16}$$

where D_{44} is calculated from

$$D_{44} = P_{45} \cdot \frac{r_{14\text{-}N_2O}}{2}. \tag{17}$$

All the parameters mentioned above are listed in Fig. 1 and defined in Table 1. Now we have all necessary parameters to separate N_2 and N_2O productions from different processes.

Similarly, $IPT_{ana N_2O}$ inherited a series of assumptions in $IPT_{classic}$, IPT_{ana} and IPT_{N_2O}. Below we list all assumptions and present how we evaluate their validity.

(1) A steady-state nitrate concentration profile across the sediment water interface must be established shortly after $^{15}NO_3^-$ addition.

(2) The parameter r_{14} (ratio of $^{15}NO_3^-$ to $^{14}NO_3^-$ undergoing denitrification) remains constant in the nitrate reduction zone resulting in ideal binomial distribution of the formed N_2O species.

(3) Denitrification is the only quantitatively significant source of ^{15}N–N_2O and is limited by the supply of NO_3^- from the overlying water.

(4) Anammox is limited by NO_3^- during $^{15}NO_3^-$ labelling experiment.

(5) The mole fraction of ^{15}N in the NO_3^- and NO_2^- pools undergoing dissimilatory reduction is equal.

(6) Nitrification is not affected by the addition of $^{15}NO_3^-$.

BGD
10, 6861–6898, 2013

Except for Assumptions 5 and 6, all the above assumptions can be evaluated via the response of ^{15}N–N_2O and ^{15}N–N_2 in the three types of incubations which will be discussed in the Sect. 4.3.

A field experiment was also conducted to evaluate the applicability of our new method and test the authenticity of the above assumptions.

4 Field experiment and assessment of IPT estimators

4.1 Sampling site and experiment design

In June 2011, sediment samples were collected from the intertidal zone of the estuary of Danshuei (25°06′38.37″ N, 121°27′52.10″ E), the largest river at northern Taiwan during low tide. The sediments are fine with a porosity of 0.76 (v/v) and moderate organic carbon content (2.3 % dry weight). Nitrate and ammonium concentrations in the overlaying water were about 30 µM and 180 µM, respectively. The water temperature is ∼ 26 °C resembling the air temperature. A total of 36 sediment cores were collected using Plexiglas tubes (30 cm long, 4.5 cm i.d.). A total of another 500 g surface sediments (top 1 cm) were taken and stored in plastic bags for slurry incubation. After sample collection, we returned to the laboratory within 2 h. Overlying water in sediment cores was adjusted to 7 cm height by carefully removing the bottom sediments. Then, the intact sediment cores were equilibrated with oxygen saturated river water at 26 °C in a tank overnight. Three types of incubations were performed following Trimmer et al. (2006).

In $^{15}NO_3^-$ concentration series experiment, we added $^{15}NO_3^-$ (100 mM, 98 ^{15}N atom%; Sigma-Aldrich) to make the overlying water of sediment cores with final concentrations of 50, 100, 150 and 200 µM and a total of 6 replicates for each concentration. All cores were sealed with overlying water been stirred by a small stir bar (located at top 4 cm) which was driven by a large external magnet (incubation tank followed the design by Trimmer et al., 2006). To ensure a constant ratio between $^{14}NO_3^-$ and $^{15}NO_3^-$ in nitrate reduction layer, a 30 min pre-incubation was set. Three replicates were sacri-

BGD
10, 6861–6898, 2013

ficed from each treatment immediately at time zero (t_0) and the rest 3 replicates were sacrificed after every 3 h of incubation at 26°, closed to in situ temperature.

The remaining 12 sediment cores were used for $^{15}NO_3^-$ time series experiments, in which all overlying waters were enriched to 50 µM of $^{15}NO_3^-$. We sacrificed 3 samples as replicates at 1 h interval starting from time zero (t_0, t_1, t_2 and t_3) over 3 h.

To subsample the sediment cores of the two above mentioned experiments, we followed protocol of Dalsgaard et al. (2000) to mix the overlying water and approximately the top 1 cm of sediments gently with a glass rod. A total of 4 mL mixed slurry was filled into a gas-tight vial (Exetainer, 12 mL) containing 100 µL of formaldehyde solution (38 % *w/v*) and a glass bead (5 mm diameter) for mixing. After capped, the headspace was quickly flushed with helium to remove unwanted air. The entire process took max. 2 min to finish. The production rates of $^{29}N_2$, $^{30}N_2$, $^{45}N_2O$ and $^{46}N_2O$ were calculated as excess ^{15}N ratio (Nielsen, 1992).

The potential activities of denitrification and anammox were measured. Following Risgaard-Petersen et al. (2004) with slight modifications. We mixed ~ 100 mL surface sediment with 100 mL of filtered (0.2 µm) river water in a beaker, and then bubbled with helium gas to remove oxygen. Anaerobic condition was confirmed by using oxygen microsensor (Unisense SA). A total of 36 slurry samples were prepared by transferring 4 mL of slurry each to gas-tight vial (Exetainer, 12 mL), and immediately purged with helium gas to ensure oxygen-free after being capped. All vials were pre-incubated overnight to allow a complete consumption of NO_3^-, NO_2^- ($^{14}NO_x^-$) and O_2. (Additional measurements confirmed NO_x^- was consumed completely after pre-incubation.) The slurries were then enriched with (1) $^{15}NH_4^+$ (the concentrated stock of 100 mM, 98 ^{15}N atom %; Sigma-Aldrich), (2) $^{15}NO_3^-$ and (3) $^{15}NH_4^+$ versus $^{14}NO_3^-$ to a final concentration of 100 µM (wet slurry). The incubations were stopped at 1 h intervals within a 3 h period by injecting 0.1 mL of formaldehyde.

BGD
10, 6861–6898, 2013

4.2 Evaluation of different versions of IPT

Experimental results were presented in Fig. 4; meanwhile, we compared N_2 and N_2O production rates derived from various IPT methods. The IPT_{anaN_2O} gave the N_2 production rate ($D'_{14\text{-}N_2}$) of $42.3 \pm 6.4\,\mu mol\,N\,m^{-2}\,h^{-1}$, which was equal to that derived from IPT_{ana}. Both IPT versions applied $r_{14\text{-}N_2O}$ with consideration of anammox in their calculations. However, overestimation in denitrification rate can be obtained by using $IPT_{classic}$ and IPT_{N_2O}. In $IPT_{classic}$, the denitrification rate, $P_{14\text{-}classic}$ ($D_{14\text{-}classic}$), was $64.9 \pm 11.2\,\mu mol\,N\,m^{-2}\,h^{-1}$ which is apparently biased due to improper $r_{14\text{-}N_2}$ and ignorance of anammox. When the $r_{14\text{-}N_2O}$ was applied to IPT_{N_2O}, the N_2 production ($D_{14\text{-}N_2}$) was $48.8 \pm 7.7\,\mu mol\,N\,m^{-2}\,h^{-1}$, which was still overestimated because of neglecting anammox. Conclusively, IPT_{ana} and IPT_{anaN_2O} provide the most appropriate estimation in considering the sole end product of N_2 from the complete denitrification.

The N_2O from the incomplete denitrification has to be taken into account in the total denitrification rate estimation, which is accomplished by IPT_{N_2O} and IPT_{anaN_2O}. Both methods gave the same N_2O production rates ($D_{14\text{-}N_2O}$) of $83.4 \pm 11.8\,\mu mol\,N\,m^{-2}\,h^{-1}$, which is two times the $D'_{14\text{-}N_2}$. The N_2O yield (production rates of N_2O relative to the total denitrification; defined as $D_{14\text{-}N_2O}/(D_{14\text{-}N_2O} + D'_{14\text{-}N_2})$) was 66 % by IPT_{anaN_2O}. This proportion is not low at all and should not be overlooked. In fact, high yield of N_2O during denitrification have been reported in the sediments of eutrophic rivers (García-Ruiz et al., 1998) and estuaries (Senga et al., 2006), where the high N_2O yield was attributed to sulphide inhibition on the last step of denitrification as Senga et al. (2006) stated. Note that, the yield number in our study remains constant for all four concentrations in the $^{15}NO_3^-$ addition experiment (slope = 0.0, $p > 0.05$) indicating that the effect of $^{15}NO_3^-$ enrichment was negligible and a homogenous incubation environment was achieved in the sediment cores. To our knowledge, Minjeaud et al. (2008) performed the only field test for IPT_{N_2O} in a coastal lagoon. In contrast to our results, they reported dramatic increase of N_2O yield from 0 % to 75 % as they increased the $^{15}NO_3^-$

BGD
10, 6861–6898, 2013

concentrations. They speculated that the analytical procedure of the isotopic composition of N_2O was not sensitivity enough in the presence of low nitrate concentrations. In our study, the nitrate concentrations were an order of magnitude higher than those in their study sites. More studies are needed to reconfirm the stable responses of N_2O yield in various environments.

N_2O contributed from unlabelled sources (P'_{44}) and labelled sources ($D_{14\text{-}N_2O}$) can both be quantified by IPT_{anaN_2O}, which provide important information in understanding the regulation factors of N_2O emission. The total production rate of N_2O ($P'_{44} + D_{14\text{-}N_2O}$) was 110 $\mu mol\,N\,m^{-2}\,h^{-1}$ in our field example. During sampling we also measured the in situ N_2O flux across air-water interface, which was 72 $\mu mol\,N\,m^{-2}\,h^{-1}$; this flux was quantified by independent method of Liss and Slater (1974). The IPT_{anaN_2O} derived N_2O production rate is higher but within the same order of magnitude with the air-water N_2O flux. Two causes may result in the difference. First, the river water carried the signal from upstream where N_2O production rate is lower. Second, the N_2O produced in sediments might eventually be reduced to N_2 during diffusion in sediments, thus the $P'_{44} + D_{14\text{-}N_2O}$ falls in-between the gross and the net N_2O production in a short time incubation. Nevertheless, this result implies that most of the N_2O produced in the sediment of the Danshuei estuary might eventually be released to the atmosphere.

The IPT_{anaN_2O} derived genuine production rate of N_2 from anammox was 13.0 ± 2.7 $\mu mol\,N\,m^{-2}\,h^{-1}$. This amount of N_2 accounts for 23 ± 4 % of genuine N_2 production (i.e. $ra = 0.23$; Fig. 5). Originally, *ra* is defined as the contribution of anammox to the total N_2 production to describe the contribution of anammox in nitrate removal processes; however, in environments with high N_2O yield, such as the Danshuei estuary, $D_{14\text{-}N_2O}$ should be included to better represent the relative net contribution of anammox. When the equation, $ra_{(N_2+N_2O)} = A_{14}/P_{14\text{-}anaN_2O}$ is applied, the ratio is reduced to 12 %. Nevertheless, our newly proposed method is more applicable to various environments such as lakes, rivers and coastal seas where had been reported as active sites

BGD
10, 6861–6898, 2013

of N_2O production (Bange et al., 1996; Seitzinger and Kroeze, 1998) and widespread occurrence of anammox (Devol, 2008).

4.3 Validate assumptions of our new IPT_{anaN_2O}

Assumptions 1 and 2 describe a continuous and stable supplying source of nitrate from overlaying water for sedimentary denitrification and anammox. If the formation of N_2O follows the binomial distribution as stated in Assumption 2, $r_{14\text{-}N_2O}$ will be an appropriate proxy referring to the constant ratio of $^{14}NO_3^-$ and $^{15}NO_3^-$ (i.e. r_{14}). In our study, the linear increase of ^{15}N-labelled N_2 and N_2O concentration in time series experiments illustrated our incubation time of 3 h was appropriate (Fig. 6a). Meanwhile, we found that the r_{14} for N_2O and N_2 maintained in a constant value during incubation period (Fig. 6b). Moreover, in our $^{15}NO_3^-$ concentration series experiment, $r_{14\text{-}N_2O}$ and $r_{14\text{-}N_2}$ decreased as a function of concentration of $^{15}NO_3^-$ added (Fig. 7a) and the maximum standard deviation was about 10 % indicating a constant r_{14} for both gases throughout the incubation. Also, the standard deviations of $r_{14\text{-}N_2O}$ are smaller than that of $r_{14\text{-}N_2}$ implying $r_{14\text{-}N_2O}$ is relatively stable. Above results indicated steady-state nitrate profiles were rebuilt both in the time series experiment and in the $^{15}NO_3^-$ concentration series experiment. This met the requirements of Assumptions 1 and 2. Previous study indicated that similar experiment took only 8 min to reach equilibrium after adding $^{15}NO_3^-$ tracer in the overlaying water in the intact sediment core incubation (Nielsen, 1992). Therefore, a 30 min pre-incubation procedure was recommended (Jensen et al., 1996; Lohse et al., 1996). However, in our experiment after pre-incubation we still need one hour to reach the constant value of r_{14} for both gases. Apparently, it required more time to reach equilibrium condition in our study environment. Noteworthy, the increment of $r_{14\text{-}N_2O}$ from t to t_1 was smaller than that of $r_{14\text{-}N_2}$, which implied that $r_{14\text{-}N_2O}$ reached to a constant earlier than $r_{14\text{-}N_2}$. We speculated that the $r_{14\text{-}N_2}$ response lag was resulted from relatively slow metabolic activity of anammox comparing with denitrification (Strous et al., 1998).

BGD
10, 6861–6898, 2013

Assumption 3, which involves $^{15}N_2O$ production, is critical in IPT_{ana}, IPT_{N_2O} and IPT_{anaN_2O} to derive accurate P_{14}. Mathematically we can resolve P_{14} by using the production of $^{15}N_2$ and $^{15}N_2O$ only if this assumption holds. Under this assumption, the "optimum" P_{14}, $P_{14\text{-}anaN_2O}$, which considers both N_2O production and $r_{14\text{-}N_2O}$, can be derived by combining Eqs. (7) and (9). Since we do not consider the possible influence of other pathways, such as chemodenitrification, dissimilatory reduction of nitrate to ammonium (DNRA) and nitrifier denitrification (see below), here we use the "optimum" for the current stage. A positive correlation between the production rate of $^{15}N_2O$ and the amount of $^{15}NO_3^-$ added (Fig. 7b) was observed in $^{15}NO_3^-$ concentration series experiment indicating that denitrification is limited by NO_3^-. We also observed a relatively constant $D_{14\text{-}N_2O}$ over various NO_3^- concentrations (Fig. 7c). Similar results were also revealed by $P_{14\text{-}ana}$ and $P_{14\text{-}anaN_2O}$ in Fig. 7d. Those observations validated that in situ N_2O production via denitrification ($D_{14\text{-}N_2O}$) was not affected by $^{15}NO_3^-$ addition as well as $P_{14\text{-}ana}$ and $P_{14\text{-}anaN_2O}$. Also, this result implied that denitrification is the only quantitatively significant source of N_2O. By contrast, the dependency of $P_{14\text{-}classic}$ on $^{15}NO_3^-$ addition (Fig. 7c) would indicate an overestimation of $P_{14\text{-}classic}$. The overestimation is attributed to the second source of ^{14}N-nitrogen, $^{14}NH_4^+$, which was converted into N_2 pool via anammox process. On the other hand, the results from anoxic slurry incubations enriched with $^{15}NH_4^+$ showed no $^{15}N_2O$ signal to support the $^{15}N_2O$ from anammox is insignificant although N_2O generated by anammox bacterial (pure strain) has been reported previously (Strous et al., 1998; van de Graaf et al., 1997). Meanwhile, our crosschecking experiment of the slurry incubations re-confirmed the occurrence of anammox, which potentially accounted for 20 % of the genuine N_2 production (data not shown).

Assumption 4 states that anammox is limited by NO_3^- as well as denitrification. We confirmed this assumption by the linear increase of A_{15} and the constant response of A_{14} as the $^{15}NO_3^-$ addition (Fig. 7e). To our knowledge, the validation of this assumption was never paid much attention (e.g. Crowe et al., 2012; Trimmer and Nicholls, 2009).

BGD
10, 6861–6898, 2013

A test on this assumption is recommended. If the results do not support it, anammox might be limited by NH_4^+. In this case, the *ra* and potential anammox activity could be estimated by slurry incubations enriched with $^{15}NH_4^+$ (Thamdrup and Dalsgaard, 2002).

Assumption 5 and 6 are indispensable for all versions of IPT, however, it is difficult to verify specifically via IPT itself. Yet, some inconsistent phenomena caused by the violation of the assumptions can be recognized as illustrated by Risgaard-Petersen et al. (2003). To simplify, the detailed descriptions are provided in Appendix B.

4.4 Uncounted nitrogen conversion pathways in IPT_{anaN_2O}

Nitrification and denitrification are assumed to be the only two processes to produce N_2O in IPT_{anaN_2O}. However, there are some other nitrogen conversion pathways we still cannot include into IPT_{anaN_2O}. For example, chemodenitrification, DNRA and nitrifier denitrification are potential N_2O producers in the field although almost all evidences in previous studies were obtained in laboratory (Brandes et al., 2007; Wrage et al., 2001). Below we illustrated the potential inference of each individual pathway if any.

Instead of measuring ^{15}N tracer signals, the P'_{44} essentially relies on $^{44}N_2O$ formation measured by IRMS (see Eq. 16). If any uncounted N_2O producing pathways from non-denitrification had occurred to an appreciable degree, the P'_{44} will be more representative of the sum of N_2O production from nitrification and other uncounted pathways. Therefore, additional experiments, such as $^{15}NH_4^+$ enrichment, are necessary to testify this parameter and reinforce our confidence. In our field example, P'_{44} was $27.0 \pm 2.7\,\mu mol\,N\,m^{-2}\,h^{-1}$ and it might has been contributed from nitrification or more exactly "non-denitrification" pathways.

Chemodenitrification represents chemical reactions that lead to the conversion of NO_x or NH_4^+ to N_2O or N_2 (Davidson, 1992; Luther et al., 1997). This process usually dominates in extreme environments, such as acidic or hydrothermal conditions (Brandes et al., 1998) and is presumably minor when compared with other microbial

BGD
10, 6861–6898, 2013

mediated processes. Once this process is proved to be important in common aquatic environments, further revision will be needed.

The observation of N_2O formation via DNRA has been proposed in pure culture (Smith and Zimmerman, 1981; Smith, 1982); again, no direct field evidence showing that DNRA is a significant N_2O source in sediment due to methodological difficulty. Although some recent studies found that DNRA is a significant source of NH_4^+ (Dong et al., 2009, 2011; Jäntti and Hietanen, 2012), we believe that the N_2O released via DNRA should be minor in most environments. The favourable conditions for DNRA are strictly anaerobic sediments where NO_3^- supply is limited. In such an environment, the complete DNRA processes with the end product of NH_4^+ might be more efficiency than the incomplete NO_3^- reduction that produces N_2O. Our idea is supported by Smith (1982) who observed a 90 % drop in N_2O production when NO_2 changes from 15 000 to 150 µM in pure stain culture. In addition, our slurry incubations showed that ^{15}N gases production accounted for maximum 100 % of added $^{15}NO_3^-$. This again suggested DNRA is insignificant in our study site. The metabolic processes of NO_3^- reducing to N_2O in denitrification and in DNRA have been demonstrated to be similar (Simon, 2002), thus, indistinguishable N_2O isotope composition between the two pathways by $^{15}NO_3^-$ tracer approach may occur. For this reason, $r_{14\text{-}N_2O}$ should be the same and still reflects the $^{14/15}N$ ratio of the consumed NO_3^- even if DNRA is an alternative significant source for the N_2O production. Therefore, rate estimations based on $r_{14\text{-}N_2O}$ should be reliable in IPT_{anaN_2O}. If DNRA produces significant N_2O, the sole inference is the estimation of $D_{14\text{-}N_2O}$, which incorporates N_2O sourced from both denitrification and DNRA.

Nitrifier denitrification is a kind of denitrification (i.e. reduction of NO_2 to N_2O) that has been demonstrated as a N_2O producing mechanism by versatile ammonia oxidizing bacteria, *Nitrosomonas* spp. (Poth and Focht, 1985). The nitrifier involves in three N_2O production pathways, namely, ammonia oxidation (the first stage of nitrification, P'_{44}), coupled nitrification-denitrification ($P_{14}n$) and nitrifier denitrification (uncounted in

BGD
10, 6861–6898, 2013

IPT_{anaN_2O}). The first two have been considered in IPT_{anaN_2O}. In terms of nitrifier denitrification, if the substrate, NO_2, purely sourced from intracellular ammonia oxidation (i.e. unlabelled NH_4^+), the product, N_2O, should be incorporated into $P_{14}n$ estimation. However, if extracellular NO_2 (i.e. $^{15}NO_2$) involves in the reaction, the "hybridized" $^{45}N_2O$ will be produced with one N atom from NH_4^+ and the other from $^{15}NO_2$. The additional "hybridized" $^{45}N_2O$ will result in the decrease of qN_2O (i.e. increase $r_{14\text{-}N_2O}$). When "hybridized" $^{45}N_2O$ contributes appreciable fraction of $^{15}N_2O$, the slope of qN_2 against qN_2O will shift toward 1 and cause a significant underestimation in *ra*. Our field experiment showed no sign of influence by "hybridized" $^{45}N_2O$. The *ra* of 23 % estimated from intact sediment cores (Fig. 5) agrees well with that from slurry incubation (20 %). This observation can be explained in two ways that either the influence of "hybridized" $^{45}N_2O$ in *ra* estimation is equal in the suboxic environment (sediment cores) and the anoxic environment (slurry) or more likely the influence of nitrifier denitrification is insignificant. Currently, our understanding of nitrifier denitrification in natural environments is limited although Wrage et al. (2005) proposed a dual-isotope labelling method to quantify N_2O production from nitrifier denitrification in soil. However, the isotope technique to identify "hybridized" $^{45}N_2O$ in the field is unavailable not mentioning quantification.

5 Conclusions and implications

Our study explored the limits of methodology for measuring nitrogen removal pathways in two aspects. First, we proposed the IPT_{anaN_2O} to accurately quantify gases production from various pathways. Secondly, our instrumental modification allows accurate measurements of the two important ^{15}N-labeled gases simultaneously from the same sample vial, which considerably reduces analytical work. The field experiments compared the results from different versions of IPT showing that IPT_{anaN_2O} is more powerful in environments with coexistence of high N_2O flux.

BGD
10, 6861–6898, 2013

In addition, our instrumental modification is potentially applicable onto high frequency on-line measurements of ^{15}N gaseous production in the flow through system (Rysgaard et al., 1994), which operates at steady-state conditions for days to weeks and is beneficial to studies on parallel processes such as assimilation, nitrification and mineralization.

Since $IPT_{ana N_2O}$ is capable of quantifying N_2O yield from denitrification and N_2O production from nitrification, this technique is specifically helpful to explore the mechanisms that regulate benthic N_2O flux. This direction of research is essential to understand the possible changes of N_2O emission in coastal eutrophication and the development of hypoxic area caused by excessive nitrogen loading.

Appendix A

Equivalence of Eqs. (13) and (15)

Below, we prove that the Eq. (13) is equal to Eq. (15). First of all, Eq. (15) can be rewritten as the following equation which represents individual datum point instead of slope from pooled data (Trimmer and Nicholls, 2009).

$$ra = \frac{2 - 2 \cdot \frac{qN_2}{qN_2O}}{2 - \frac{qN_2}{qN_2O}}. \quad \text{(A1)}$$

On the other hand, Eq. (13) is

$$ra = \frac{A_{14}}{D'_{14\text{-}N_2} + A_{14}}. \quad \text{(A2)}$$

BGD
10, 6861–6898, 2013

By substituting D'_{14} and A_{14} with Eqs. (5) and (6), respectively, we can express *ra* as

$$ra = \frac{P_{29} - 2 \cdot r_{14\text{-}N_2O}}{P_{29} + P_{30} \cdot (1 - r_{14\text{-}N_2O})}. \quad \text{(A3)}$$

Since P_{29}/P_{30} equals to $2 \cdot r_{14\text{-}N_2O}$, the *ra* can be expressed in terms of r_{14} after the numerator and the denominator being divided by P_{30}, which is

$$ra = \frac{2 \cdot r_{14\text{-}N_2} - 2 \cdot r_{14\text{-}N_2O}}{2 \cdot r_{14\text{-}N_2} - r_{14\text{-}N_2O} + 1}. \quad \text{(A4)}$$

Substituting r_{14} with q using Eq. (14), and arranging the equation, we get Eq. (A1).

Appendix B

Discussions of Assumption 5 and 6

Assumption 5 assumes NO_3^- reduction is the only source of NO_2^- in anoxic sediment layer, that is, supplies from other potential sources, such as NO_2^- from ammonia oxidation or downward diffusion from overlying water, are insignificant. Under this assumption, the fraction of ^{15}N in nitrite will be equal to nitrate. This assumption is indispensable for all versions of IPT; however, it is difficult to test specifically via IPT itself (see below). Several studies focused particularly on NO_2^- production showed that NO_2^- in anoxic sediment is mainly resulted from NO_3^- reduction (De Beer, 2000; Meyer et al., 2005; Stief et al., 2002), which supports this assumption. Although it is untestable via IPT itself, some phenomena caused by the violation of the assumption can be recognized if slurry incubation is conducted.

Under condition of high anammox activity and significant NO_2^- supply from non-labelled sources to anammox, inconsistent outcomes will be obtained between incubations of intact core and slurry sediment. For example, a significant anammox activity

BGD
10, 6861–6898, 2013

can be revealed in slurry incubation after adding $^{15}NH_4^+$; meanwhile, a positive correlation between values of $D_{14\text{-classic}}$ and $^{15}NO_3^-$ concentrations should be obtained from intact core experiment if all NO_2^- comes from labelled sources (e.g. Fig. 7c). On the contrary, if NO_2^- is largely supplied from non-labelled sources a constant value of $D_{14\text{-classic}}$ will be obtained in $^{15}NO_3^-$ concentration series experiment because N_2 produced from anammox will be supported by non-labelled NO_2^-. Note that the violation of Assumption 6 below might result in the same inconsistency.

In general, nitrification which uses NH_4^+ as the substrate will not be affected by the addition of $^{15}NO_3^-$ (Assumption 6). However, an indirect effect might happen in NO_3^- addition experiment since high $^{15}NO_3^-$ concentration may stimulate anammox activity to deplete NH_4^+ thus limiting nitrification as a consequence. The decreased nitrification therefore diminishes the NO_3^- supply resulting in an underestimation of $P_{14}n$, the genuine gases production via coupled nitrification-denitrification. The underestimation of $P_{14}n$ of course leads to underestimate of $D_{14\text{-classic}}$. Apparently, higher $^{15}NO_3^-$ additions will cause larger degree of underestimation in $D_{14\text{-classic}}$. On the other hand, if this is the case anammox must be traceable; oppositely, the $^{29}N_2$ produced from anammox will cause the overestimation of $D_{14\text{-classic}}$. This overestimation of $D_{14\text{-classic}}$ is also enlarged as increasing $^{15}NO_3^-$ additions. To summarise, the underestimation of $D_{14\text{-classic}}$ caused by diminishing nitrification will be compensated by stimulating anammox in different $^{15}NO_3^-$ treatments. Such compensation blocks a good positive correlation between $D_{14\text{-classic}}$ and the concentration of $^{15}NO_3^-$ spike. Coupled with significant anammox activity observed in slurry incubation by adding NH_4^+, phenomena observed here thus resembles that caused by the violation of Assumptions 5.

Supplementary material related to this article is available online at: http://www.biogeosciences-discuss.net/10/6861/2013/bgd-10-6861-2013-supplement.pdf.

BGD
10, 6861–6898, 2013

Acknowledgements. This research was supported by the National Science Council, Taiwan (NSC 100-2621-M-001-003-MY3) and the National Natural Science Foundation of China (NSFC 41176059 and B07034).

References

Bange, H. W.: New directions: the importance of oceanic nitrous oxide emissions, Atmos. Environ., 40, 198–199, 2006.

Bange, H. W., Rapsomanikis, S., and Andreae, M. O.: Nitrous oxide in coastal waters, Global Biogeochem. Cy., 10, 197–207, 1996.

Bergsma, T. T., Ostrom, N. E., Emmons, M., and Robertson, G. P.: Measuring simultaneous fluxes from soil of N_2O and N_2 in the field using the ^{15}N-gas "nonequilibrium" technique, Environ. Sci. Technol., 35, 4307–4312, 2001.

Brandes, J. A., Boctor, N. Z., Cody, G. D., Cooper, B. A., Hazen, R. M., and Yoder, H. S.: Abiotic nitrogen reduction on the early Earth, Nature, 395, 365–367, 1998.

Brandes, J. A., Devol, A. H., and Deutsch, C.: New developments in the marine nitrogen cycle, Chem. Rev., 107, 577–589, 2007.

Crowe, S. A., Canfield, D. E., Mucci, A., Sundby, B., and Maranger, R.: Anammox, denitrification and fixed-nitrogen removal in sediments from the Lower St. Lawrence Estuary, Biogeosciences, 9, 4309–4321, doi:10.5194/bg-9-4309-2012, 2012.

Dalsgaard, T., Nielsen, L. P., Brotas, V., Viaroli, P., Underwood, G. J. C., Nedwell, D. B., Sundbäck, K., Rysgaard, S., Miles, A., Bartoli, M., Dong, L. F., Thornton, D. C. O., Ottosen, L. D. M., Castaldelli, G., and Risgaard-Petersen, N.: Protocol Handbook for NICE-Nitrogen Cycling in Estuaries, National Environmental Research Institute, Copenhagen, Denmark, 2000.

Davidson, E. A.: Sources of nitric oxide and nitrous oxide following wetting of dry soil, Soil Sci. Soc. Am. J., 56, 95–102, 1992.

De Beer, D.: Potentiometric microsensors for in situ measurements in aquatic environments, in: In Situ Monitoring of Aquatic Systems: Chemical Analysis and Speciation, edited by: Buffle, J. and Horvai, G., Wiley, 161–194, 2000.

BGD
10, 6861–6898, 2013

Devol, A. H.: Denitrification including anammox, in: Nitrogen in the Marine Environment, 2nd edn., edited by: Capone, D., Bronk, D., Mulholland, M., and Carpenter, E., Elsevier, Amsterdam, 263–301, 2008.

Dong, L. F., Smith, C. J., Papaspyrou, S., Stott, A., Osborn, A. M., and Nedwell, D. B.: Changes in benthic denitrification, nitrate ammonification, and anammox process rates and nitrate and nitrite reductase gene abundances along an estuarine nutrient gradient (the Colne Estuary, UK), Appl. Environ. Microb., 75, 3171–3179, 2009.

Dong, L. F., Sobey, M. N., Smith, C. J., Rusmana, I., Phillips, W., Stott, A., Osborn, A. M., and Nedwell, D. B.: Dissimilatory reduction of nitrate to ammonium, not denitrification or anammox, dominates benthic nitrate reduction in tropical estuaries, Limnol. Oceanogr., 56, 279–291, 2011.

García-Ruiz, R., Pattinson, S. N., and Whitton, B. A.: Denitrification and nitrous oxide production in sediments of the Wiske, a lowland eutrophic river, Sci. Total Environ., 210, 307–320, 1998.

Groffman, P. M., Altabet, M. A., Böhlke, J. K., Butterbach-Bahl, K., David, M. B., Firestone, M. K., Giblin, A. E., Kana, T. M., Nielsen, L. P., and Voytek, M. A.: Methods for measuring denitrification: diverse approaches to a difficult problem, Ecol. Appl., 16, 2091–2122, 2006.

Jäntti, H. and Hietanen, S.: The effects of hypoxia on sediment nitrogen cycling in the Baltic Sea, AMBIO, 41, 161–169, 2012.

Jensen, K. M., Jensen, M. H., and Kristensen, E.: Nitrification and denitrification in Wadden Sea sediments (Konigshafen, Island of Sylt, Germany) as measured by nitrogen isotope pairing and isotope dilution, Aquat. Microb. Ecol., 11, 181–191, 1996.

Joye, S. B. and Anderson, I. C.: Nitrogen cycling in coastal sediments, in: Nitrogen in the Marine Environment, 2nd edn., edited by: Capone, D. G., Bronk, D. A., Mulholland, M. R., and Carpenter, E. J., Academic Press, Amsterdam, 868–915, 2008.

Liss, P. S. and Slater, P. G.: Flux of gases across the air-sea interface, Nature, 247, 181–184, 1974.

Lohse, L., Kloosterhuis, H. T., Van Raaphorst, W., and Helder, W.: Denitrification rates as measured by the isotope pairing method and by the acetylene inhibition technique in continental shelf sediments of the North Sea, Mar. Ecol-Prog. Ser., 132, 169–179, 1996.

Luther III, G. W., Sundby, B., Lewis, B. L., Brendel, P. J., and Silverberg, N.: Interactions of manganese with the nitrogen cycle: alternative pathways to dinitrogen, Geochim. Cosmochim. Ac., 61, 4043–4052, 1997.

BGD
10, 6861–6898, 2013

Master, Y., Shavit, U., and Shaviv, A.: Modified isotope pairing technique to study N transformations in polluted aquatic systems: theory, Environ. Sci. Technol, 39, 1749–1756, 2005.
McIlvin, M. R. and Casciotti, K. L.: Fully automated system for stable isotopic analyses of dissolved nitrous oxide at natural abundance levels, Limnol. Oceanogr.-Meth., 8, 54–66, 2010.
Meyer, R. L., Risgaard-Petersen, N., and Allen, D. E.: Correlation between anammox activity and microscale distribution of nitrite in a subtropical mangrove sediment, Appl. Environ. Microb., 71, 6142–6149, 2005.
Minjeaud, L., Bonin, P. C., and Michotey, V. D.: Nitrogen fluxes from marine sediments: quantification of the associated co-occurring bacterial processes, Biogeochemistry, 90, 141–157, 2008.
Mulder, A., Graaf, A. A., Robertson, L. A., and Kuenen, J. G.: Anaerobic ammonium oxidation discovered in a denitrifying fluidized bed reactor, FEMS Microbiol. Ecol., 16, 177–184, 1995.
Naqvi, S. W. A., Bange, H. W., Farías, L., Monteiro, P. M. S., Scranton, M. I., and Zhang, J.: Marine hypoxia/anoxia as a source of CH_4 and N_2O, Biogeosciences, 7, 2159–2190, doi:10.5194/bg-7-2159-2010, 2010.
Nielsen, L. P.: Denitrification in sediment determined from nitrogen isotope pairing, FEMS Microbiol. Lett., 86, 357–362, 1992.
Poth, M. and Focht, D. D.: ^{15}N kinetic analysis of N_2O production by *Nitrosomonas europaea*: an examination of nitrifier denitrification, Appl. Environ. Microb., 49, 1134–1141, 1985.
Risgaard-Petersen, N., Nielsen, L. P., Rysgaard, S., Dalsgaard, T., and Meyer, R. L.: Application of the isotope pairing technique in sediments where anammox and denitrification coexist, Limnol. Oceanogr.-Meth., 1, 63–73, 2003.
Risgaard-Petersen, N., Meyer, R. L., Schmid, M., Jetten, M. S. M., Enrich-Prast, A., Rysgaard, S., and Revsbech, N. P.: Anaerobic ammonium oxidation in an estuarine sediment, Aquat. Microb. Ecol., 36, 293–304, 2004.
Rysgaard, S., Risgaard-Petersen, N., Sloth, N. P., Jensen, K., and Nielsen, L. P.: Oxygen regulation of nitrification and denitrification in sediments, Limnol. Oceanogr., 39, 1643–1652, 1994.
Seitzinger, S. P. and Kroeze, C.: Global distribution of nitrous oxide production and N inputs in freshwater and coastal marine ecosystems, Global Biogeochem. Cy., 12, 93–113, 1998.
Senga, Y., Mochida, K., Fukumori, R., Okamoto, N., and Seike, Y.: N_2O accumulation in estuarine and coastal sediments: the influence of H_2S on dissimilatory nitrate reduction, Estuar. Coast. Shelf S., 67, 231–238, 2006.

BGD
10, 6861–6898, 2013

Simon, J.: Enzymology and bioenergetics of respiratory nitrite ammonification, FEMS Microbiol. Rev., 26, 285–309, doi:10.1111/j.1574-6976.2002.tb00616.x, 2002.
Smith, M. S.: Dissimilatory Reduction of NO_2^- to NH_4^+ and N_2O by a soil *Citrobacter* sp., Appl. Environ. Microb., 43, 854–860, 1982.
Smith, M. S. and Zimmerman, K.: Nitrous oxide production by nondenitrifying soil nitrate reducers, Soil Sci. Soc. Am. J., 45, 865–871, 1981.
Spott, O., Russow, R., Apelt, B., and Stange, C. F.: A ^{15}N-aided artificial atmosphere gas flow technique for online determination of soil N_2 release using the zeolite Köstrolith SX6®, Rapid Commun. Mass Sp., 20, 3267–3274, 2006.
Stevens, R. J., Laughlin, R. J., Atkins, G. J., and Prosser, S. J.: Automated determination of nitrogen-15-labeled dinitrogen and nitrous oxide by mass spectrometry, Soil Sci. Soc. Am. J., 57, 981–988, 1993.
Stief, P., De Beer, D., and Neumann, D.: Small-scale distribution of interstitial nitrite in freshwater sediment microcosms: the role of nitrate and oxygen availability, and sediment permeability, Microb. Ecol., 43, 367–377, 2002.
Strous, M., Heijnen, J. J., Kuenen, J. G., and Jetten, M. S. M.: The sequencing batch reactor as a powerful tool for the study of slowly growing anaerobic ammonium-oxidizing microorganisms, Appl. Microbiol. Biot., 50, 589–596, 1998.
Thamdrup, B. and Dalsgaard, T.: Production of N_2 through anaerobic ammonium oxidation coupled to nitrate reduction in marine sediments, Appl. Environ. Microb., 68, 1312–1318, 2002.
Trimmer, M. and Nicholls, J. C.: Production of nitrogen gas via anammox and denitrification in intact sediment cores along a continental shelf to slope transect in the North Atlantic, Limnol. Oceanogr., 54, 577–589, 2009.
Trimmer, M., Risgaard-Petersen, N., Nicholls, J. C., and Engström, P.: Direct measurement of anaerobic ammonium oxidation (anammox) and denitrification in intact sediment cores, Mar. Ecol.-Prog. Ser., 326, 37–47, 2006.
van de Graaf, A. A., de Bruijn, P., Robertson, L. A., Jetten, M. S. M., and Kuenen, J. G.: Metabolic pathway of anaerobic ammonium oxidation on the basis of ^{15}N studies in a fluidized bed reactor, Microbiology, 143, 2415, 1997.
Wrage, N., Velthof, G. L., van Beusichem, M. L., and Oenema, O.: Role of nitrifier denitrification in the production of nitrous oxide, Soil Biol. Biochem., 33, 1723–1732, 2001.

BGD
10, 6861–6898, 2013

Wrage, N., van Groenigen, J. W., Oenema, O., and Baggs, E. M.: A novel dual-isotope labelling method for distinguishing between soil sources of N_2O, Rapid Commun. Mass Sp., 19, 3298–3306, doi:10.1002/rcm.2191, 2005.

BGD
10, 6861–6898, 2013

Table 1. List of abbreviations used in equations.

Abbreviations	Definitions
P_{29}	Production rate of $^{29}N_2$ determined with excess ^{15}N ratio
P_{30}	Production rate of $^{30}N_2$ determined with excess ^{15}N ratio
P_{45}	Production rate of $^{45}N_2O$ determined with excess ^{15}N ratio
P_{46}	Production rate of $^{46}N_2O$ determined with excess ^{15}N ratio
$[D_{44} + P'_{44}]_{IRMS}$	Production rate of $^{44}N_2O$ calculated as signal area (concentration) change of *m/z* 44 with time
r_{14}	Ratio between $^{14}NO_3^-$ and $^{15}NO_3^-$ undergoing nitrate reduction
$r_{14\text{-}N_2}$	Estimator of r_{14}, based on $^{15}N_2$ production
$r_{14\text{-}N_2O}$	Estimator of r_{14}, based on $^{15}N_2O$ production
$r_{14}w$	Ratio between $^{14}NO_3^-$ and $^{15}NO_3^-$ in the water column
q	Fraction of ^{15}N in NO_3^- pool undergoing reduction
qN_2	Estimator of q, based on $^{15}N_2$ production
qN_2O	Estimator of q, based on $^{15}N_2O$ production
$D_{14\text{-classic}}$	Denitrification N_2 production rate by reactions using $^{14}NO_3^-$ as substrate estimated with $IPT_{classic}$
$D_{14\text{-}N_2}$	Denitrification N_2 production rate by reactions using $^{14}NO_3^-$ as substrate estimated with IPT_{N_2O}
$D'_{14\text{-}N_2}$	Denitrification N_2 production rate by reactions using $^{14}NO_3^-$ as substrate excluding anammox
D_{14-N_2O}	Denitrification N_2O production rate by reactions using $^{14}NO_3^-$ as substrate
D_{44}	$^{44}N_2O$ production rate via denitrification
A_{14}	Anammox N_2 production rate supported with $^{14}NO_3^-$
A_{15}	Anammox N_2 production rate supported with $^{15}NO_3^-$
$P_{14\text{-classic}}$	Genuine N_2 production rate estimated with $IPT_{classic}$, equal to $D_{14\text{-classic}}$
$P_{14\text{-ana}}$	Genuine N_2 production rate estimated with IPT_{ana}
$P_{14\text{-}N_2O}$	Genuine N_2 and N_2O production rate estimated with IPT_{N_2O}
$P_{14\text{-ana}N_2O}$	Genuine N_2 and N_2O production rate estimated with IPT_{anaN_2O}
$P_{14}w$	Genuine N_2 and N_2O production rate supported by the nitrates from water column
$P_{14}n$	Genuine N_2 and N_2O production rate supported via coupled nitrification
ra	Contribution of anammox to N_2 production
$ra_{(N_2+N_2O)}$	Contribution of anammox to N_2 and N_2O production
P'_{44}	Production rate of N_2O via nitrification

BGD
10, 6861–6898, 2013

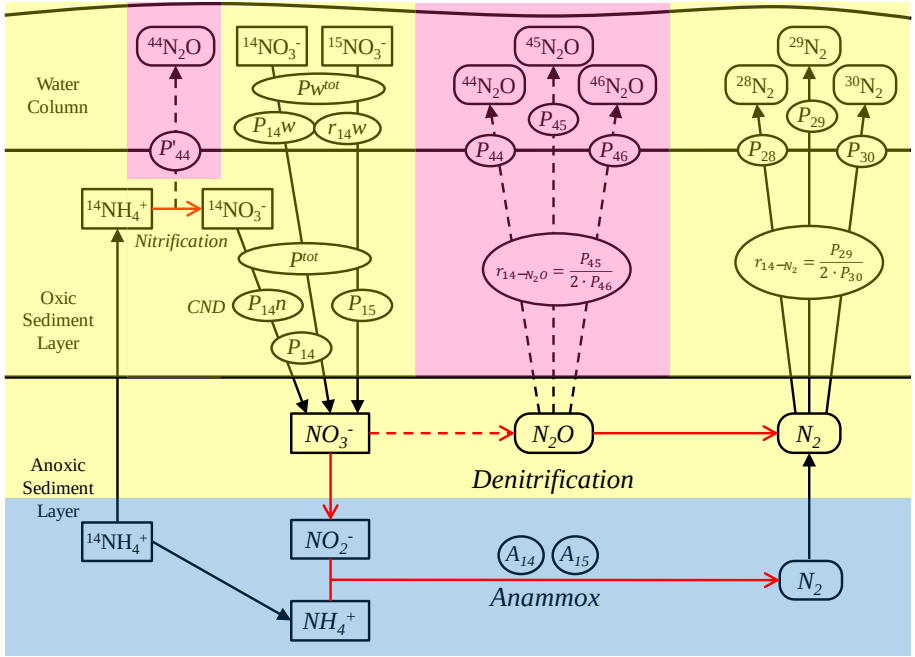

Fig. 1. Schematic diagram of various N transformation processes and rates considered by different versions of IPT (after ref. 11). Yellow plate represents $IPT_{classic}$. Yellow and blue plates represent IPT_{ana}. Yellow and pink plates represent IPT_{N_2O}. Full diagram represent IPT_{anaN_2O}. Gases isotopic N_2 and/or N_2O production rates in individual process are designated by "P_x^y" or "A_x" (in mole unit, e.g. $\mu mol\,m^2\,h^{-1}$). Detailed explanation of the abbreviations is given in Table 1. The equations of $r_{14\text{-}N_2}$ and $r_{14\text{-}N_2O}$ represent the ratio between using $^{14}NO_3^-$ and $^{15}NO_3^-$ during nitrate reduction in different estimators. CND is the process of coupled nitrification denitrification.

BGD
10, 6861–6898, 2013

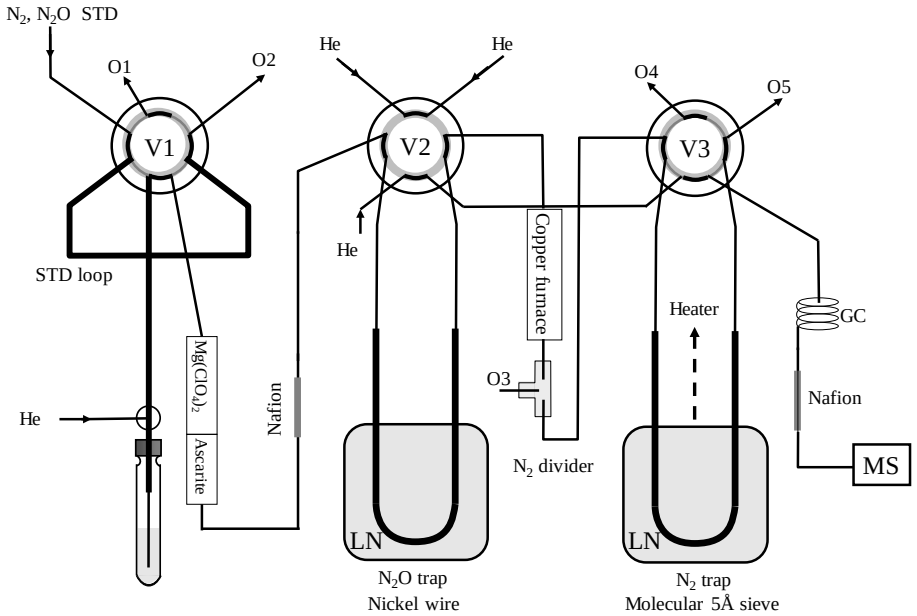

Fig. 2. Schematic diagram of pre-concentration system at sample loading phase: GC, gas chromatogram column (ConFlow); He, helium; LN, liquid nitrogen; MS, mass spectrometer; O1-5, outlets to atmosphere; STD, standard gas; V1-3, automated control valves. Please refer to text for details.

BGD
10, 6861–6898, 2013

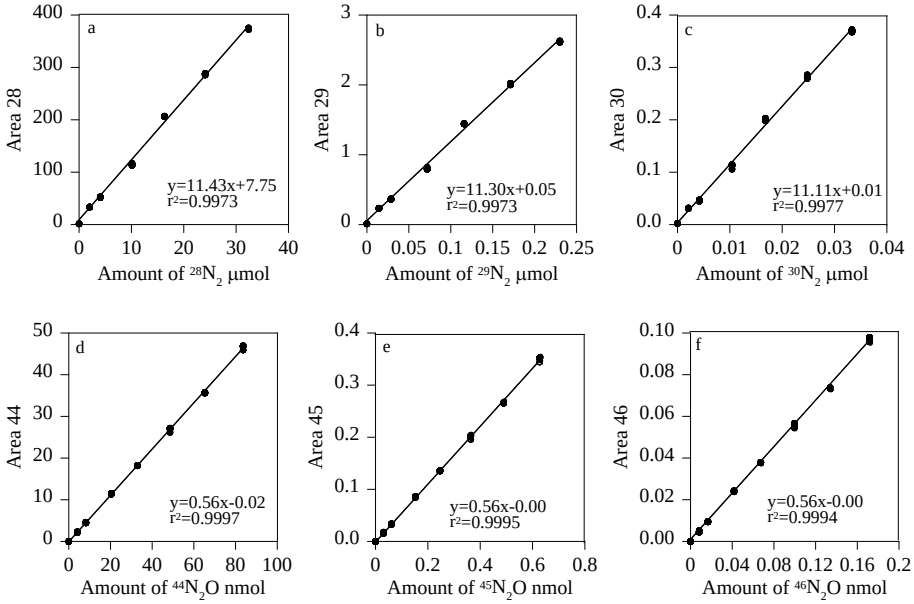

Fig. 3. (a–c) Linear responses of signal area *m/z* 28, 29, 30 against given amounts of standard gas $^{28}N_2$, $^{29}N_2$ and $^{30}N_2$, respectively. **(d–f)** Linear responses of signal area *m/z* 44, 45, 46 to various amounts of stand gas $^{44}N_2O$, $^{45}N_2O$ and $^{46}N_2O$, respectively.

BGD
10, 6861–6898, 2013

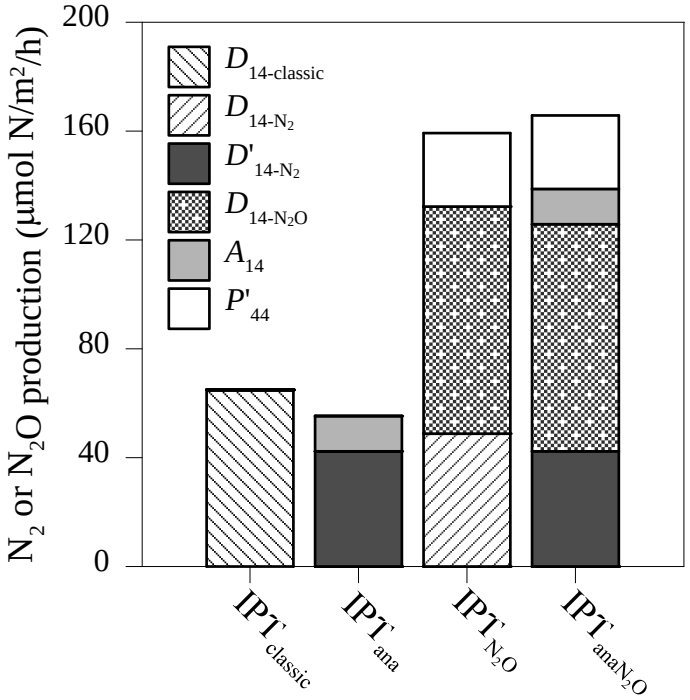

Fig. 4. Comparison of N_2 or N_2O production rates estimated by different versions of IPT.

BGD
10, 6861–6898, 2013

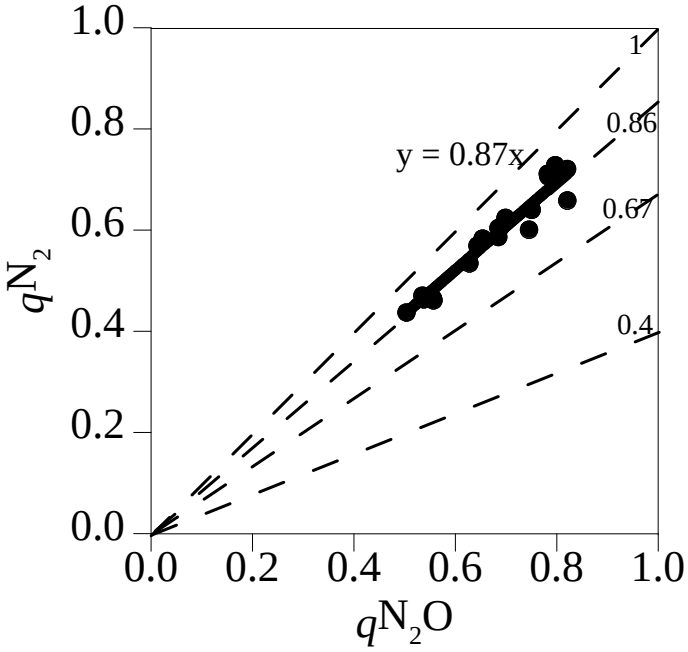

Fig. 5. The plot of qN_2 vs. qN_2O from concentration series incubations. Dashed lines represent the theoretical slope of 1, 0.86, 0.67 and 0.40, which corresponding to *ra* of 0 %, 25 %, 50 % and 75 %, respectively. The slope of regression is 0.87 ± 0.03 (r^2 = 0.95, $p < 0.05$, n = 21) corresponding to *ra* of 23 ± 4 %.

BGD
10, 6861–6898, 2013

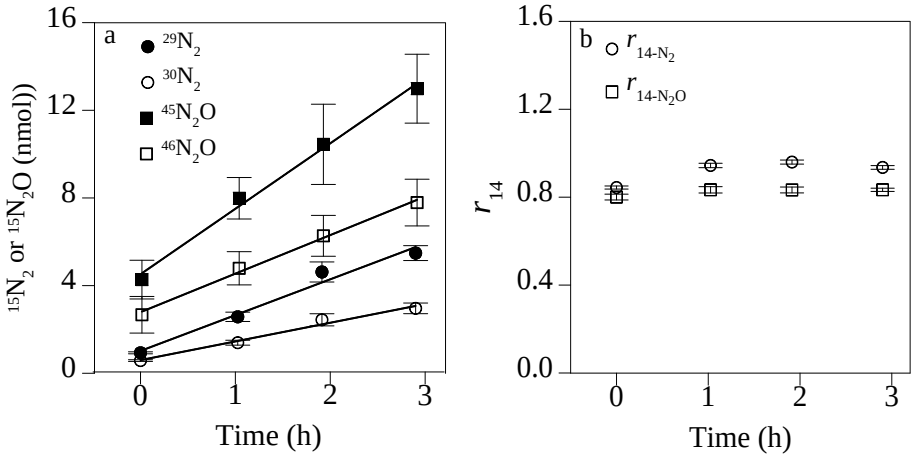

Fig. 6. Results from time series experiment. **(a)** Production of $^{15}N_2$ and $^{15}N_2O$ as a function of time. Regression coefficients (r^2) are 0.97, 0.98, 0.99 and 0.99 for $^{29}N_2$, $^{30}N_2$, $^{45}N_2O$ and $^{46}N_2O$, respectively. **(b)** Observational $r_{14\text{-}N_2}$ and $r_{14\text{-}N_2O}$ values as a function of time. Values are means ± 1 SEM (n = 3).

BGD
10, 6861–6898, 2013

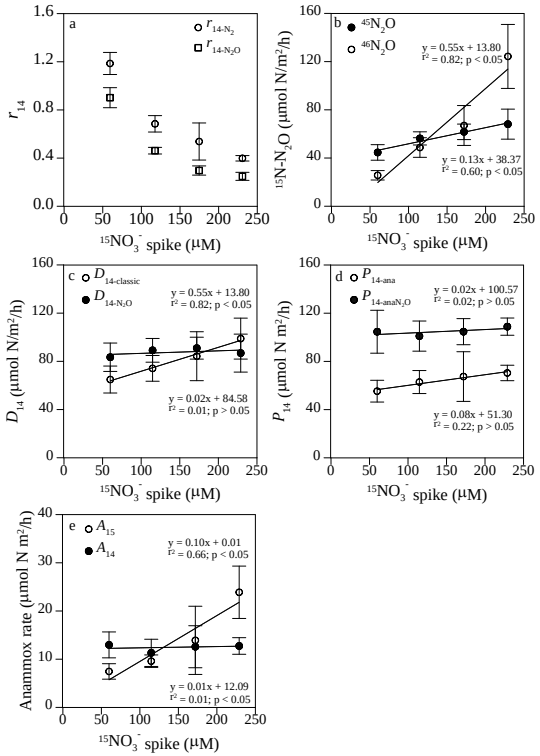

Fig. 7. Results from concentration series experiment. **(a)** r_{14} as a function of $^{15}NO_3^-$ spike; **(b)** production of $^{15}N_2O$ as a function of $^{15}NO_3^-$ spike; **(c)** comparison of denitrification N_2 production rates estimated by $IPT_{classic}$ ($D_{14\text{-classic}}$) and IPT_{N_2O} ($D_{14\text{-}N_2O}$); **(d)** comparison of genuine N_2 and N_2O production rates estimated by IPT_{ana} ($P_{14\text{-ana}}$) and IPT_{anaN_2O} ($P_{14\text{-anaN}_2O}$); **(e)** the labeled (A_{15}) and unlabeled (A_{14}) anammox rates as a function of $^{15}NO_3^-$ spike. Values are means ± 1 SEM (n = 3). Regression analysis used individual data (n = 12).

BGD
10, 6861–6898, 2013